

# Optical Engineering

OpticalEngineering.SPIEDigitalLibrary.org

## **Distributed high-precision time transfer through passive optical networks**

Guiling Wu  
Liang Hu  
Hao Zhang  
Jianping Chen

**SPIE.**

# Distributed high-precision time transfer through passive optical networks

Guiling Wu,\* Liang Hu, Hao Zhang, and Jianping Chen

Shanghai Jiao Tong University, State Key Laboratory of Advanced Optical Communication Systems and Networks, Department of Electronic Engineering, Shanghai 200240, China

**Abstract.** We propose a one-point to multipoint distributed time transfer through passive optical networks using a time division multiple access (TDMA) based two-way time transfer. The clock at each clock user node is, in turn, compared with the high-precision reference clock at a master node by a two-way time transfer during assigned subperiods. The corresponding TDMA control protocol and time transfer units for the proposed scheme are designed and implemented. A  $1 \times 8$  experimental system with a 20 km single-mode fiber in each subpath is demonstrated. The results show that a standard deviation of  $<60$  ps can be reached in each comparison subperiod. © 2014 Society of Photo-Optical Instrumentation Engineers (SPIE) [DOI: 10.1117/1.OE.53.9.096113]

Keywords: distributed time transfer; optical fiber; two-way time comparison; passive optical networks.

Paper 141069 received Jul. 9, 2014; revised manuscript received Aug. 23, 2014; accepted for publication Sep. 2, 2014; published online Sep. 23, 2014.

## 1 Introduction

Time transfer over optical fiber links has attracted extensive interest due to its advantages of high stability, broad bandwidth, low loss, and so on. Up until now, several point-to-point fiber-optic time transfer systems have been demonstrated.<sup>1-4</sup> Śliwczyński et al. demonstrated that it is possible to achieve a single-picosecond accuracy in the point-to-point fiber-optic bidirectional time/frequency transfer over a 60 km fiber when only considering the effects resulting from the fiber alone.<sup>3</sup> Many practical applications, however, require a distributed time transfer, where a common time reference should be transferred to all user clock nodes (UCNs).<sup>5</sup> The distributed time transfer over coaxial cable or satellite channels presents disadvantages, such as susceptibility to transmission interference, high loss, low stability, etc., and thus has limited range and precision.<sup>6</sup> Laufl et al. proposed a distributed time transfer over optical fiber links with electrical distributors.<sup>7</sup> Although an optical fiber link has a better performance than coaxial cable or satellite channels in terms of transmission distance and stability, the employment of electrical distributors leads to extra electrical noise. Moreover, as active devices, they need to be maintained in the operation and O/E/O conversion has to be used for the connection to fiber. Several network-based time transfer techniques such as network time protocol and precise time protocol can also support distributed time transfer. However, their precision is limited to a magnitude of several nanoseconds.<sup>8,9</sup>

In this paper, we propose a one-point to multipoint distributed time transfer scheme over a passive optical networks (PON).<sup>10</sup> The clock at each user node is, in turn, compared with the high-precision reference clock at the master node by a time division multiple access (TDMA) based two-way time transfer mechanism. The TDMA control mechanism and corresponding time transfer units for the distributed two-way time transfer are designed and implemented. A  $1 \times 8$  time transfer experimental system with a standard deviation

(Stdev) of  $<60$  ps in every comparison subperiod is demonstrated.

## 2 Distributed Time Transfer Scheme

Figure 1 illustrates the system architecture of the proposed distributed time transfer over PONs, where a master clock node (MCN) is connected to several UCNs through an optical distributed network (ODN). According to the practical application requirements and scenarios, a private distributed time transfer system with different topologies such as star and tree can be built. The proposed scheme can also be implemented in an existing commercial PON via wavelength division multiplexing technology to provide the distributed time transfer service. Bidirectional optical amplifiers can be used on sublinks to extend the transmission distances.<sup>4,11</sup>

The designed TDMA mechanism for the proposed distributed time transfer is shown in Fig. 2. The whole procedure operates periodically under the control of the MCN. Each synchronization period is divided into a series of subperiods with each corresponding to a UCN. In each subperiod, a connection between the corresponding UCN and the MCN is built with an “Establish” procedure. After that, a point-to-point two-way time transfer between the clocks at the UCN and the MCN is carried out. When the comparison precision or time is reached, the two-way time transfer between the two node ends and the connection between them is disconnected with a “Remove” procedure.

Figure 3 shows the flowchart diagram of the proposed distributed time transfer scheme. The processing steps in each synchronization period are as follows:

1. The MCN takes the current UCN according to a certain sequence, and enters the corresponding subperiod.
2. There are three processing phases in each subperiod.

Phase 1: The MCN periodically broadcasts a connection request containing the address of the current

\*Address all correspondence to: Guiling Wu, E-mail: wuguilin@sjtu.edu.cn

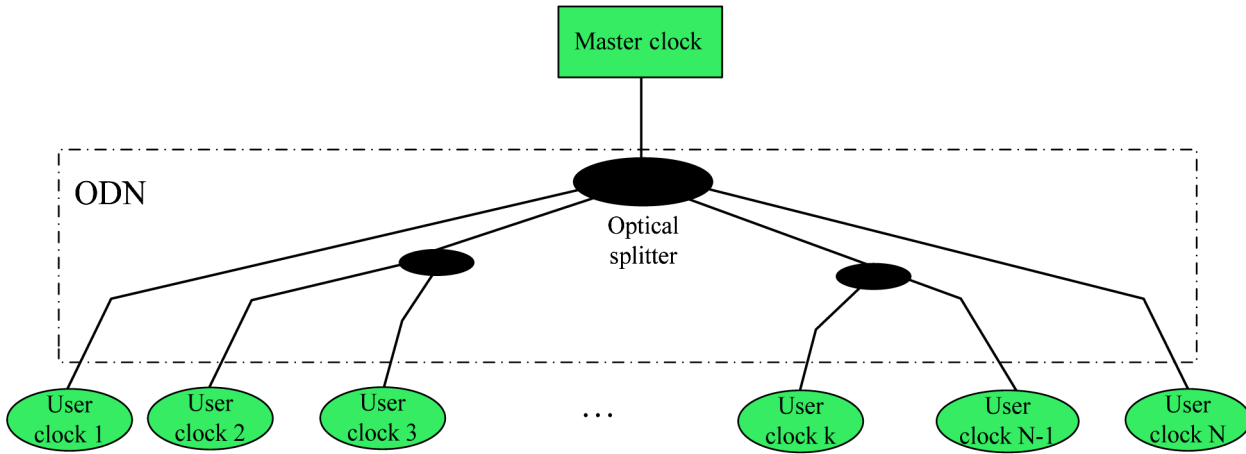


Fig. 1 The architecture of the proposed distributed time transfer over an optical fiber.

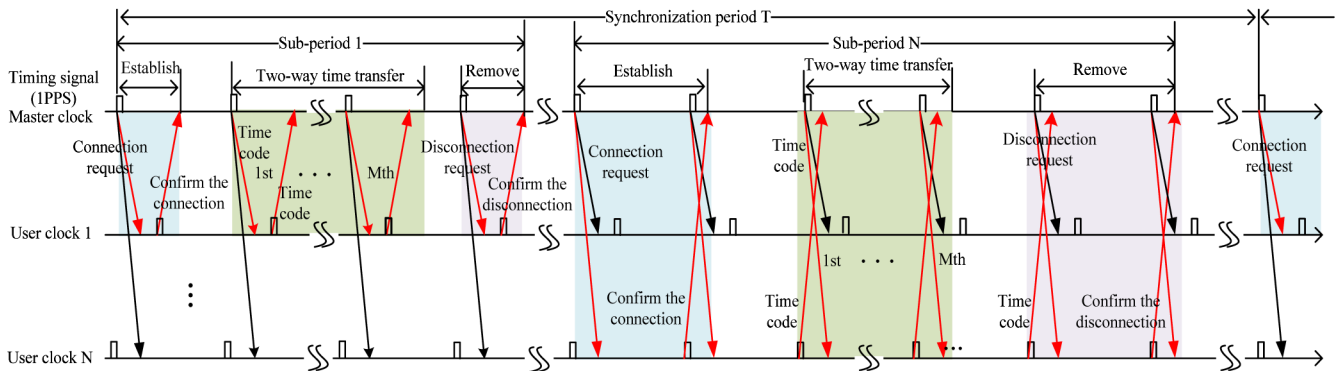


Fig. 2 The time division multiple access control mechanism for the distributed time transfer scheme.

UCN to all UCNs through the ODN until it receives a connection confirmation or the maximum connection request time (require\_limit) is reached. When the MCN receives a connection confirmation, it confirms that the connection between the MCN and the current UCN has been established. If the MCN does not receive a connection confirmation after sending the connection request in require\_limit, it reads that the current UCN is lost, and goes to step 3. At the user side, the UCN whose local address is the same as the destination address in the received connection request replies with a connection confirmation to the MCN for each received connection request.

Phase 2: The MCN and the current UCN encode the local time scales (1 pps) into time codes and send them to each other along the optical fiber link established in phase 1. At the same time, the two nodes recover the 1 pps from the received time code and measure the time difference between the local 1 pps and the recovered 1 pps. The current UCN calculates its clock difference to the MCN according to the two-way time transfer principle<sup>2</sup>

$$\Delta T = 1/2\{(T_{MU} - T_{UM}) + (\tau_F^{MU} - \tau_F^{MU}) + (\tau_T^M - \tau_T^U + \tau_R^U - \tau_R^M)\}, \quad (1)$$

where  $T_{MU}$  ( $T_{UM}$ ) is the time difference measured by the TIC at the MCN (UCN);  $\tau_F^{MU}$  ( $\tau_F^{UM}$ ) is the propagation delay of the optical fiber link from the MUN to UCN (the UCN to MCN);  $\tau_T^M$  ( $\tau_R^M$ ) and ( $\tau_T^U$ ) ( $\tau_R^U$ ) are the forward (backward) time delays of the MCN and UCN, respectively.

Phase 3: When the designated comparison time or precision is reached, the MCN stops transmission of the time code and sends disconnection requests to the current UCN. If the MCN receives a disconnection confirmation or the disconnection requiring times is greater than the require\_limit, go to 3. At the UCN side, the current user stops transmission of the time code, replies a disconnection confirmation, and turns off the transmitting laser once it receives a disconnection request.

3. If the current UCN is the last one, go to 1. Otherwise, take the next UCN as the current UCN, go to 2.

### 3 Experimental Results

Figure 4 schematically shows the  $1 \times 8$  experimental setup. The length of the optical fiber between the MCN and each UCN is about 20 km. Each node mainly includes a TDM controller, a codec, and a small form-factor pluggable (SFP) transceiver. The TDMA controller is used to realize the TDMA control described in Sec. 2, generate and parse

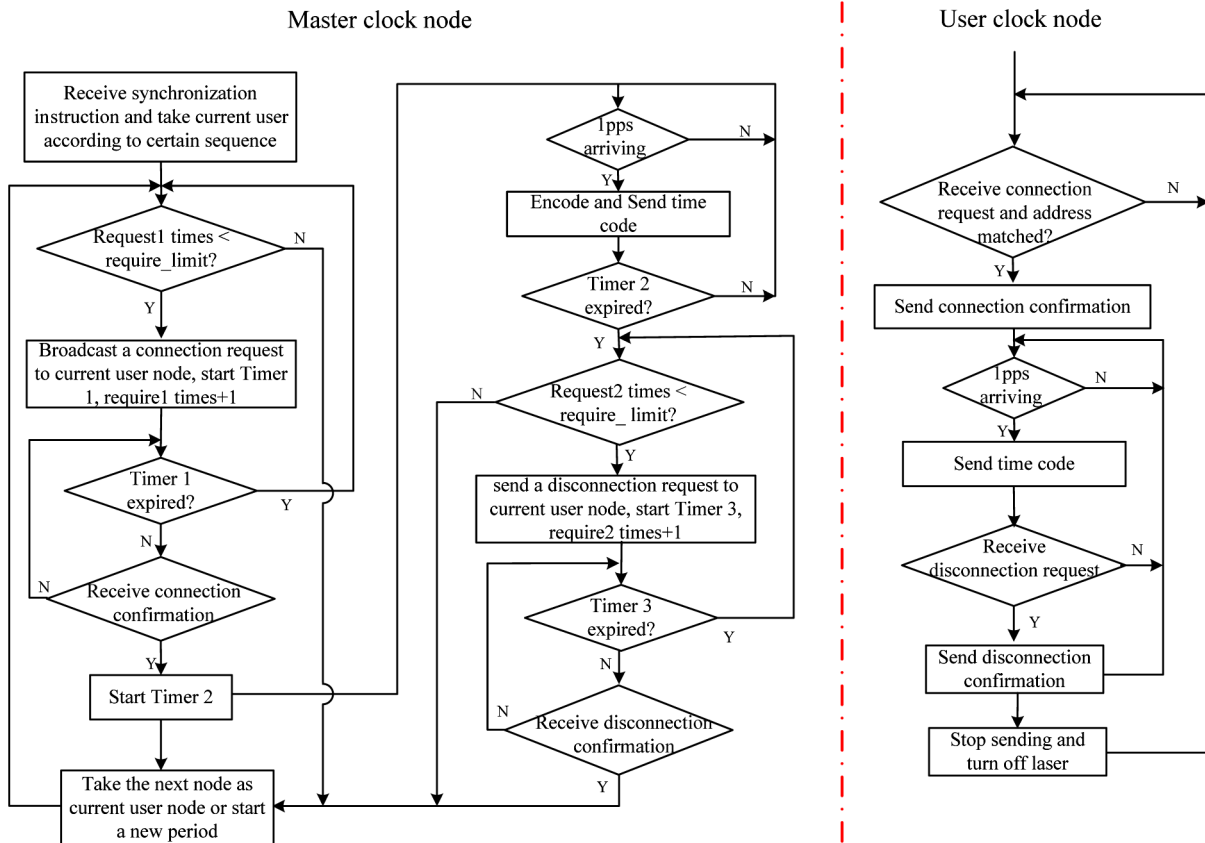


Fig. 3 The flowchart diagram of the proposed distributed time transfer scheme.

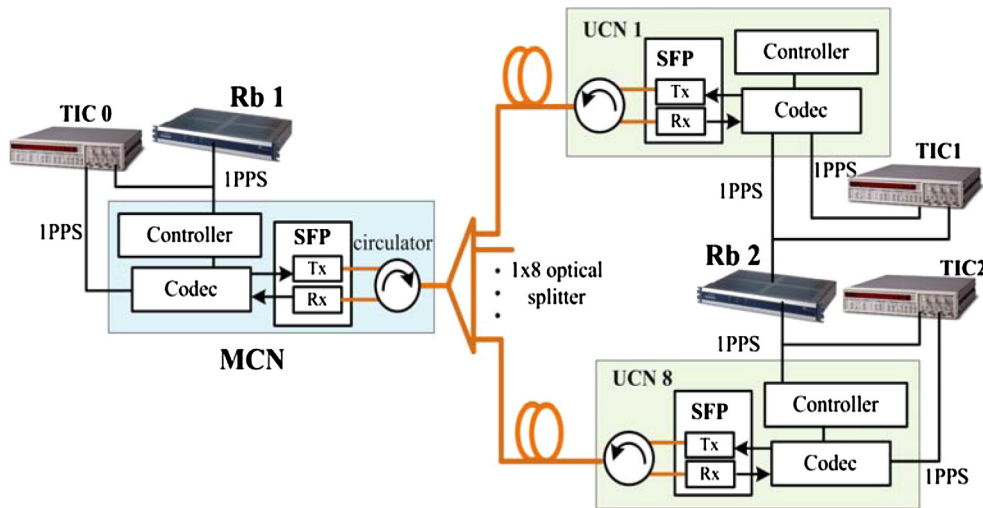


Fig. 4 The experimental setup for the proposed distributed time transfer.

control frames for the TDM-based time transfer. The codec is responsible for encoding the 1 pps from the local clock into a time code and decoding the received time code to recover the 1 pps from the remote node. The SFP transceiver is used to transmit/receive the time codes into/from the fiber link. The difference of the launched wavelengths of SFPs in the bidirection is set within 0.1 nm to reduce the asymmetry induced by the fiber dispersion as much as possible. At each node, the time difference between the local 1 pps and the recovered

1 pps is measured by a time interval counter (TIC) (Stanford Research Systems, Sunnyvale, California, SR620).

In order to be transmitted directly using commercial optical transceivers for optical communications and carry more time transfer information such as measured time differences, a modified Inter-Range Instrumentation Group (IRIG)-B time code, shown in Fig. 5, is adopted in the experimental system. Compared to the standard IRIG-B,<sup>12</sup> the modified time code keeps the pulse-width coding rule of the standard

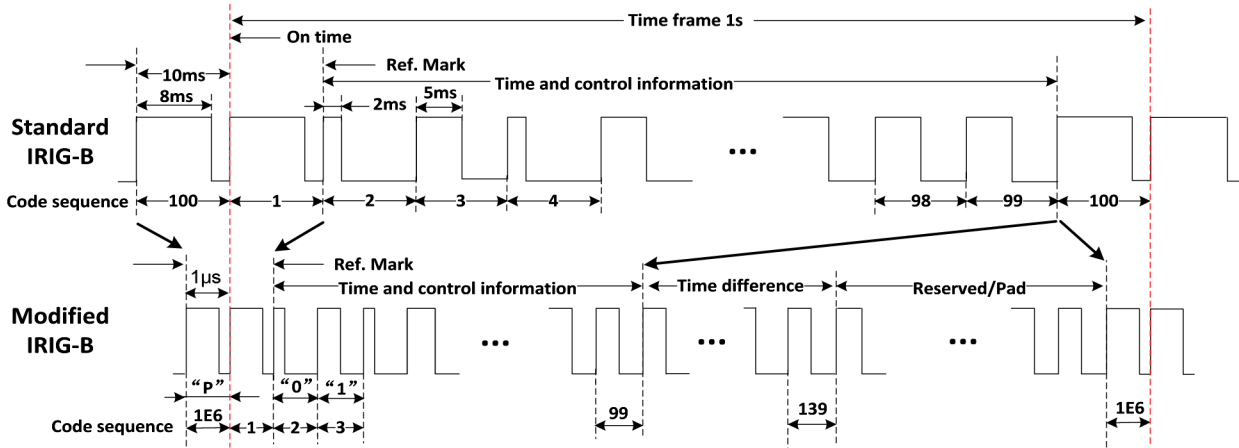


Fig. 5 The modified IRIG-B time code format.

IRIG-B while increasing its bit rate to 1 Mb/s by compressing its index count interval (the time interval between the leading edges of two consecutive bits) from 10 ms to 1  $\mu$ s. The definitions of the first 99 bits and the last bit in the modified IRIG-B frame are the same as those in the standard IRIG-B for carrying the 1 pps flag, which are the time and control information defined in the standard IRIG-B. The 40 bits following the first 99 bits are defined as the time difference field used to carry the measured time difference between the local 1 pps signal and the recovered 1 pps signal. The rest of the 999860 bits in the modified IRIG-B frame are reserved for user-defined information such as the calibrated and/or measured values on line, which are padded with “binary 1” pulses with a duration of 50% of the index count interval when they are not used.

Figure 6 shows the state machine of the TDMA controller at the MCN and UCN. At the MCN, see Fig. 6(a), the machine enters the “Init” state from “idle” while the TDMA controller receives a synchronous instruction. After completing the initiation processing and configuration, the control unit enters the “Req\_Connect” to generate and send a Req\_Connect frame, including the current UCN address to all UCNs, then enters “Wait” state. Upon receiving a Conf\_Connect before the designated duration, it enters the “Send time code” state from the “Wait” state; if the designated duration expires, it enters the “Fail\_1” state. In the “Fail\_1” state, if the connection request times are less than the require\_limit times, it enters the “Req\_Connect”

state again; otherwise, it transits to the “Next” state. In the “Send timecode” state, the controller instructs the Codec to start two way time transfer processing, and steps into the “Req\_Disconnect” state when the designated comparison maximum times or precision is reached. In the “Req\_Disconnect” state, the controller sends a Req\_Disconnect frame and enters the “Wait” state. In the “Wait” state, the controller enters the “Next” state when receiving a Conf\_Disconnect before a designated duration. If the designated duration is expired, it enters the “Fail\_2” state. In the “Fail\_2” state, if the disconnection request times are less than the require\_limit, it enters the “Req\_Disconnect” state again; otherwise, it transits to the “Next” state. In the “Next” state, it updates the current node and steps into the “Req\_Connect” again. At each UCN, see Fig. 6(b), the controller enters from the “Idle” state to the “Conf\_Connect” state to send a connection confirmation to the MCN state upon receiving a Req\_Connect frame including the local address. In the “Send time code” state, the controller instructs the Codec to start the two-way time transfer with the MCN. After receiving a disconnection request, it enters the “Conf\_Disconnect” state, where the controller replies a disconnection confirmation to the MCN and then goes to the “Idle” state. If the designated maximum comparison times are reached, the controller automatically goes to the “Idle” state.

The performance of the distributed time transfer system is first evaluated in the case where all nodes are connected to a

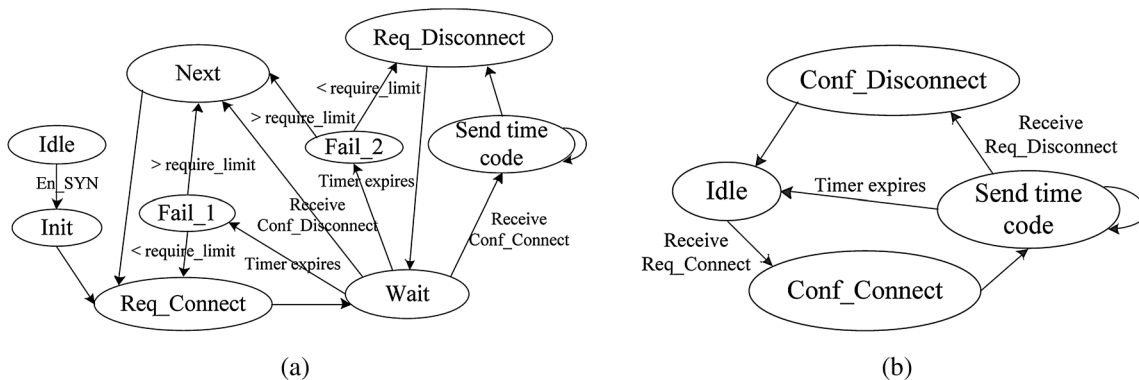
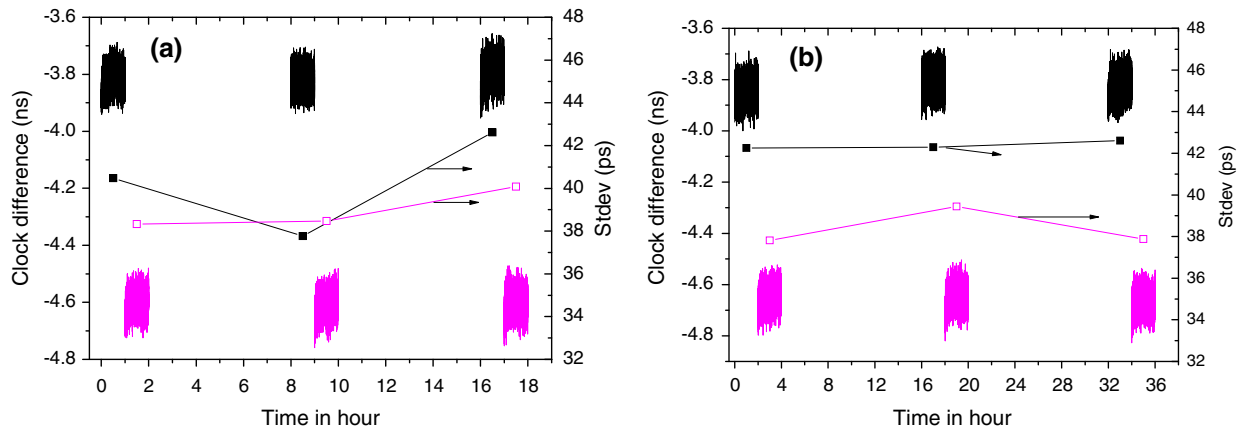
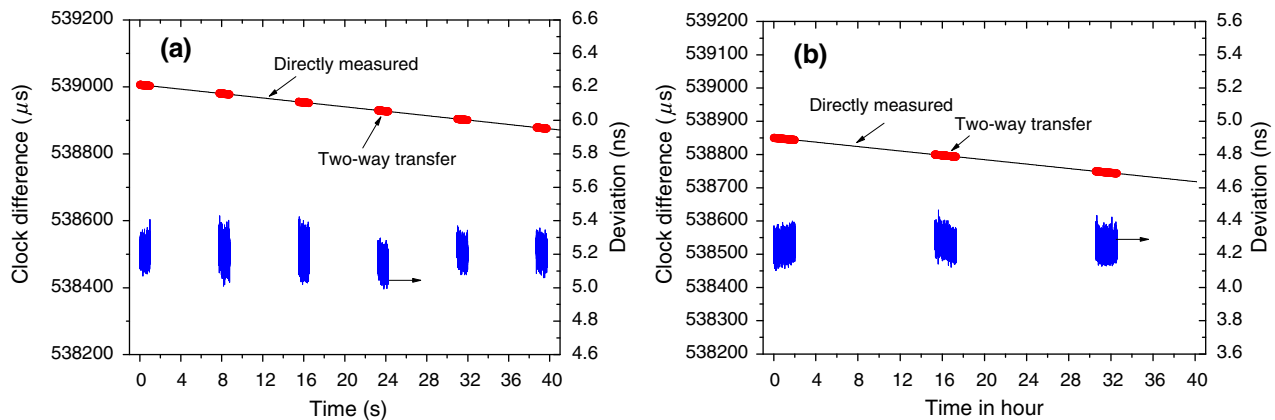


Fig. 6 The state transition process of the controller at the master clock node (a) and user clock node (b).



**Fig. 7** The measured clock difference and the calculated Stdevs while all nodes are connected to a common clock. (a) The subperiod is 1 h and (b) the subperiod is 2 h.



**Fig. 8** The measured clock difference and its deviation to “accurate” values while two nodes are connected to different clocks. (a) The subperiod is 1 h and (b) the subperiod is 2 h.

common rubidium (Rb) clock (Symmetricom, San Jose, California, 8040C) to eliminate the effect of the jitter and drift of the clock on the measurement. The Rb clock has a stability less than  $1.5E-11/s$  and outputs a 1 pps with a rise time  $<20$  ns. Figure 7 shows the clock differences of two UCNs relative to the MCN obtained by two-way time transfers when the subperiod is 1 and 2 h, respectively. In this figure, the TDMA based two-way time transfer with the corresponding subperiod can be observed, which is coincident with the TDMA control mechanism described in Sec. 2. One can also see that the clock differences are not zero (about  $-3.8$  and  $-4.6$  ns for the two UCNs, respectively) even when all three nodes are connected to a common Rb clock. The difference mainly comes from the asymmetry of the propagation delay of the cables and the time transfer units at difference nodes, which can be mitigated by calibration. The delay asymmetry caused by the bidirectional wavelength difference of about 0.1 nm on a 20 km optical fiber is  $<40$  ps. The Stdev of the measured time differences during each comparison subperiod is also shown in Fig. 7. We can see that a Stdev of  $<60$  ps can be achieved in every comparison subperiod.

Figure 8 shows the clock difference between a UCN and the MCN connected to two different Rb clocks (Symmetricom, 8040C, and precise time & frequency, Inc., Wakefield, ptf 3203A) obtained by the two-way time

transfer when the subperiod is 1 and 2 h, respectively. The ptf 3203A has a stability less than  $3E-11/s$ , and outputs a 1 pps with a rise time  $<6$  ns. The clock difference between the two clocks is also directly measured by a TIC and is shown in this figure. The difference between the two clock differences, which reflects the deviation of the clock difference obtained by the two-way optical time transfer to the “accurate” clock difference, is also shown in this figure. One can see that the deviations during the comparison subperiods have almost the same average value, which is mainly related to the asymmetry of the propagation delay of the cables and the time transfer units at two nodes, and which can be calibrated. The Stdev of the deviation during each comparison subperiod is also  $<60$  ps.

#### 4 Conclusion

In this paper, we proposed a distributed time transfer scheme over a one-point to multipoint optical passive network by combining TDMA and a two-way optical fiber time transfer. The TDMA control mechanism and corresponding time transfer units for the distributed two-way time transfer are designed and implemented. A  $1 \times 8$  distributed time transfer experimental system is demonstrated with a single-mode fiber span over 20 km. The result shows that a Stdev of time difference  $<60$  ps can be achieved in every comparison subperiod.

In comparison with the point-to-point configuration, the proposed scheme is cost-effective and easy to put into practical applications. Although the distance of each sublink is limited by the optical power splitting among multiple paths, the reachable sum distance of all sublinks will be at the same level as that of the point-to-point fiber-optic time transfer since passive optical splitters will not introduce additional noise. Moreover, the distance can be extended by using optical amplifiers on the sublink or reducing the output port number of optical splitters. Optical splitters with different splitting ratios can also be used to satisfy the practical requirement of users at different distances.

It should be noted that the time transfer between each UCN and the MCN is only performed during the assigned subperiod. The clock at a UCN should have enough frequency stability to satisfy the specific application requirements during subperiods that are not assigned to the UCN. Accordingly, the clock differences of a UCN to the MCN during subperiods not assigned to it can be predicted on the measured clock differences during the latest subperiod assigned to it by certain prediction algorithms.<sup>13,14</sup>

### Acknowledgments

This work was supported in part by the National Natural Science Foundation of China (61127016 and 61107041), SRFDP of MOE (Grant No. 20130073130005).

### References

1. S. R. Jefferts et al., "Two-way time and frequency transfer using optical fibers," *IEEE Trans. Instrum. Meas.* **46**(2), 209–211 (1997).
2. V. Smotlacha, A. Kuna, and W. Mache, "Time transfer in optical network," in *Proc. 42th Annual PTTI Meeting*, Reston, Virginia (2010).
3. Ł. Śliwczyński, P. Krehlik, and M. Lipiński, "Optical fibers in time and frequency transfer," *Meas. Sci. Technol.* **21**(7), 075302 (2010).
4. Ł. Śliwczyński and J. Kołodziej, "Bidirectional optical amplification in long-distance two-way fiber-optic time and frequency transfer systems," *IEEE Trans. Instrum. Meas.* **62**(1), 252–262 (2013).
5. L. E. Primas, T. R. Logan Jr., and G. F. Lutes, "Applications of ultra-stable fiber optic distribution systems," in *Proc. of the 43rd Annual Symp. on Frequency Control*, Denver, CO, pp. 202–211 (1989).
6. W. Lewandowski, J. Azoubib, and W. J. Klepczynski, "GPS: primary tool for time transfer," *Proc. IEEE* **87**(1), 163–172 (1999).
7. J. Lafl et al., "Clocks and timing in the NASA deep space network," in *Proc. of the 2005 IEEE Int. Frequency Control Symposium and Exposition*, Vancouver, BC, pp. 830–835 (2005).
8. L. De Vito, S. Rapuano, and L. Tomaciello, "One-way delay measurement: state of the art," *IEEE Trans. Instrum. Meas.* **57**(12), 2742–2750 (2008).
9. R. L. Scheiterer et al., "1  $\mu$ s-conform line length of the transparent clock mechanism defined by the precision time protocol (PTP version 2)," in *Proc. IEEE ISPCS*, Ann Arbor, MI, pp. 92–97 (2008).
10. R. P. Davey et al., "Long-reach passive optical networks," *J. Lightwave Technol.* **27**(3), 273–291 (2009).
11. C. Delisle and J. Conradi, "Model of bidirectional transmission in an open cascade of optical amplifiers," *J. Lightwave Technol.* **15**(5), 749–757 (1997).
12. Timing Committee Telecommunications and Timing Group, "IRIG Serial Time Code Formats," Secretariat Range Commanders Council, U.S. Army White Sands Missile Range, New Mexico, IRIG standard 200-04 (2004).
13. A. I. Dounis et al., "A comparison of grey model and fuzzy predictive model for time series," *World Acad. Sci. Eng. Technol.* **2**(6), 1064–1069 (2008).
14. Z. Zheng, Y. Chen, and X. Lu, "An improved grey model and its application research on the prediction of real-time GPS satellite clock errors," *Chin. Astron. Astrophys.* **33**(1), 72–89 (2009).

**Guiling Wu** received his BS degree from Haer Bing Institute of Technology in 1995, and his MS and PhD degrees from Huazhong University of Science and Technology in 1998 and 2001, respectively. Now he is an associate professor at the State Key Laboratory on Advanced Optical Communication Systems and Networks, Shanghai Jiao Tong University. His research interests include photonic signal processing and transmission, and optical networking.

**Liang Hu** received his master's degree from Shanghai Jiao Tong University in 2014. His research focuses on the fiber-optic time and frequency transfer.

**Hao Zhang** received his BSc degree from Xian Jiao Tong University in 2012. He is currently working toward the PhD degree in optical communications at Shanghai Jiao Tong University. His research focuses on fiber-optic time and frequency transfer.

**Jianping Chen** received his BSc degree from Zhejiang University in 1983, and MSc and PhD degrees from Shanghai Jiao Tong University in 1986 and 1992, respectively. Now he is a professor at the State Key Laboratory on Advanced Optical Communication Systems and Networks, Department of Electronic Engineering, Shanghai Jiao Tong University. His main research topics cover photonic devices and subsystems, optical networking, and sensing optics.